J Mater Sci: Mater Med (2006) 17:911–918
DOI 10.1007/s10856-006-0180-0

An impedance study of two types of stainless steel in Ringer physiological solution containing complexing agents

Mojca Slemnik · Ingrid Milošev

Received: 23 May 2005 / Accepted: 23 August 2005

Abstract The effect of complexing agents EDTA and citric acid on the electrochemical behaviour of AISI 304 and orthopaedic stainless steels in Ringer physiological solution was investigated by potentiodynamic polarization method and electrochemical impedance spectroscopy (EIS). The content of Mo has a pronounced effect on the corrosion resistance, as evident by the broader passive range of the orthopaedic stainless steel containing Mo. The addition of complexing agents induces significant changes in polarization and impedance characteristics, i.e., the shift of corrosion and breakdown potentials in a more negative direction, an increase in current density, and a significant decrease in charge transfer resistance. The results were interpreted by the formation of soluble complexes of metal ions with chelating agents, especially EDTA, which suppressed the formation of the outer Fe(III) layer of the passive film. The impact of complexing agent on the electrochemical parameters was found to be related to its concentration in electrolyte and the stability constant of the complex formed with the related metal ion.

1. Introduction

The application of implants made of stainless steel into the human body dates back to the 1920s [1]. Today stainless steel is one of the most frequently used metallic biomaterials for short-term internal fixation devices, and for long-term total hip replacements. It exhibits favourable combination of mechanical properties, corrosion resistance and cost effectiveness [1]. Stainless steels have numerous applications not only in biomedical applications but also in the technological field. In all of these applications their corrosion resistance is essential and was extensively investigated. In neutral or slightly alkaline solutions, passivity is established due to the formation of a complex oxide film containing a Cr-oxide inner layer and a Fe-oxide rich outer layer [2–8]. The composition of the outer layer depends on the potential and changes from Fe_3O_4 and $Fe(OH)_2$ in the lower potential range to Fe_2O_3 and FeOOH at more positive potentials. Nickel is depleted in the oxide layer but is enriched in the metal surface beneath [5, 8]. Molybdenum, on the other hand, is enriched in the passive oxide layer. The effect of molybdenum has been studied by numerous authors and its beneficial effect on pitting corrosion resistance is well documented [9–18]. Several theories have been proposed about the role of Mo but they can be basically divided into two categories concerning effects during active dissolution [10–13] and effects on the passive film [14, 15] [more references in 9].

The *in vitro* studies performed under simulated physiological conditions were mostly devoted to an improvement in the corrosion resistance of stainless steel by applying various surface treatments [19–21], or changing the composition of the bulk alloy [22–24]. The latter seems to be more efficient since it was shown that high nitrogen content is beneficial for localized corrosion [23, 24]. Okazaki et al. [25] studied the corrosion resistance of various implant alloys in a pseudo physiological solution by polarization curves and X-ray photoelectron spectroscopy (XPS). Milošev and Strehblow [8], on the other hand, used XPS to investigate the composition of the oxide films formed on orthopaedic and AISI 304 stainless

M. Slemnik
Faculty of Chemistry and Chemical Engineering, Department of Physical Chemistry, University of Maribor, Smetanova 17, 2000 Maribor, Slovenia

I. Milošev (✉)
Jožef Stefan Institute, Department of Physical and Organic Chemistry, Jamova 39, 1000 Ljubljana, Slovenia, and Orthopaedic Hospital Valdoltra, Jadranska c. 31, 6280 Ankaran, Slovenia

steels as a function of electrode potential in Hank's simulated physiological solution with and without the addition of citrate. Due to their complexation ability citrate ions were used to mimic the role of proteins as *in vivo* biomolecules. The addition of citrate significantly affected the passivation behaviour of orthopaedic and AISI 304 stainless steels because it changed the distribution of the elements within the passive layer and at the metal surface beneath [8]. The latter process is due to an increased dissolution in the presence of citrate, as studied in detail by electrochemical methods [26]. Similar findings were reported for non-physiological conditions, i.e. iron in a borate buffer containing EDTA [27], low-carbon steel in a borate buffer containing citrate [28], iron in a borate buffer containing 2,2'-bipyridine [29] and As-Sb alloys in the presence of citric acid [30].

In the present work the behaviour of orthopaedic stainless steel and AISI 304 stainless steel is investigated in Ringer physiological solution with and without the addition of complexing agents EDTA and citric acid using polarization curves and electrochemical impedance spectroscopy (EIS).

2. Experimental

The materials tested were a commercial stainless steel AISI 304, denoted as sample A, (Goodfellow, Cambridge Ltd., UK) and stainless steel used for the manufacture of total hip replacements. The latter samples, denoted as samples B, were cut out from the femoral head of a total hip replacement (Protema 42, Protek, Sulzer, Winterthur, Switzerland) and correspond to ASTM F138-1986 [31]. The composition of the samples, mainly differing in the content of molybdenum and nickel, was confirmed by EDS:

sample A (AISI 304): 18.7 Cr, 9.0 Ni, 0.14 Mo, 0.93 Si, 1.4 Mn, Fe balance;

sample B (orthopaedic): 18.1 Cr, 14.2 Ni, 2.66 Mo, 0.34 Si, 1.6 Mn, Fe balance.

The samples were cut in the shape of discs with 12 mm diameter and 4 mm thickness. They were mechanically polished with 600, 800, 1000 and 1200 abrasive SiC papers and fine polished with diamond pastes to a mirror-like finish. The samples were degreased in acetone.

The measurements were performed at 37°C in a standard 300 ml-Tacussel glass cell with the specimen as a working electrode, the platinum counterelectrode and a saturated calomel electrode (SCE) as a reference electrode. All the potentials in the text refer to the SCE scale. The measurements were performed in a Ringer solution (8.60 g NaCl, 0.3 g KCl and 0.33 g $CaCl_2 \cdot 2H_2O$ in 1 L) commercialized by B. Braun, Melsungen, Germany. The addition of complexing agents EDTA (ethylendiaminetetraacetic acid disodium salt dihydrate) and citric acid at concentrations 0.01 M and 0.05 M was studied in the Ringer solution. After the addition of complexing agents the pH value was adjusted to the physiological value by the addition of dissolved NaOH.

Potentiodynamic anodic polarization curves were recorded using a PAR & EG&G potentiostat/galvanostat Model 263 and Softcorr software. Curves were recorded at a scan rate of 1 mV s^{-1} starting from the potential value 250 mV more negative than the corrosion potential, E_{corr}. Electrochemical impedance spectroscopy (EIS) measurements were performed using a Solartron 1287 Electrochemical Interface and a Solartron 1250 Frequency response analyser. Data were collected using CorrWare and Zplot software and interpreted with CorrView and ZView software developed by Scribner Associates, Inc. EIS measurements were carried out after a 10 min polarization at a given potential in a frequency range from 60 kHz down to 0.001 Hz, with the excitation voltage amplitude of 30 mV.

3. Results

3.1. Anodic polarization curves in Ringer solution with and without complexing agents

For the sake of comparison, anodic polarization curves of two stainless steels investigated and individual metal components, Fe, Cr, Ni and Mo, are given in Fig. 1. Iron metal shows the corrosion potential, E_{corr}, at −0.35 V followed by a short passive region extending from −0.30 to −0.10 V. Nickel shows an anodic peak at −0.08 V followed by an increase in current density at 0.12 V. Molybdenum exhibits no

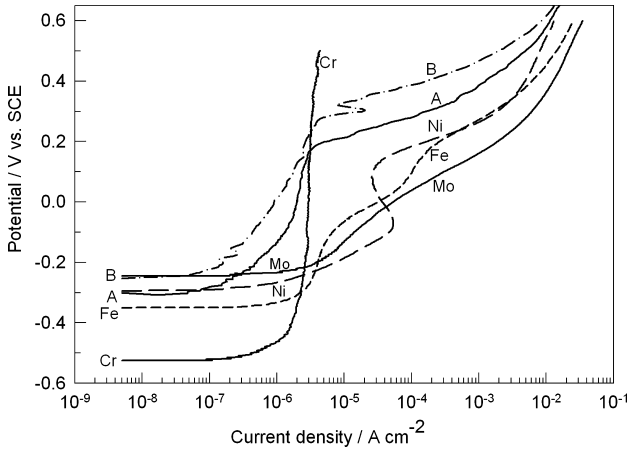

Fig. 1 Potentiodynamic curves for individual metals, Fe, Cr, Ni and Mo, and AISI 304 (A) and orthopaedic (B) stainless steels in Ringer physiological solution. dE/dt = 1 mVs^{-1}.

Table 1 Values of corrosion (E_{corr}) and breakdown potential (E_b) for AISI 304 (A) and orthopaedic (B) stainless steels in Ringer solution with and without the addition of EDTA and citric acid

	Ringer solution	+0.01 M citric acid	+0.01 M EDTA	+0.05 M citric acid	+0.05 M EDTA
Sample A E_{corr} (V)	−0.17	−0.27	−0.31	−0.39	−0.42
Sample B E_{corr} (V)	−0.21	−0.27	−0.35	−0.37	−0.44
Sample A E_b (V)	0.20	0.19	0.18	0.16	0.10
Sample B E_b (V)	0.32	0.30	0.25	0.20	0.22

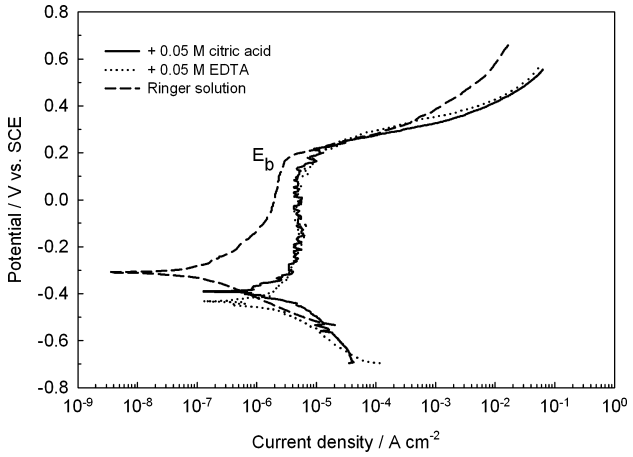

Fig. 2 Potentiodynamic curves for AISI 304 stainless steel (A) in Ringer physiological solution with and without addition of EDTA and citric acid. dE/dt = 1 mV s^{-1}.

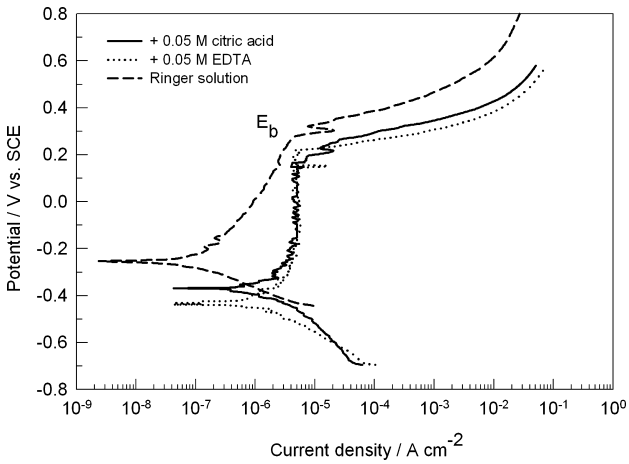

Fig. 3 Potentiodynamic curves for orthopaedic stainless steel (B) in Ringer physiological solution with and without addition of EDTA and citric acid. dE/dt =1 mVs^{-1}.

tendency towards passivation with current density increasing steadily with potential. On the contrary, chromium metal shows a broad passive region extending from −0.45 V to 0.50 V. Both stainless steel samples show lower corrosion resistance than Cr metal but higher compared to other metals. Although Mo itself shows no tendency towards passivation, its incorporation in the passive film formed on stainless steel is beneficial for resistance to pitting corrosion, as already investigated extensively [9–18, 32]. The breakdown potential, E_b, denoting the beginning of current density increase in the passive range, is for 120 mV more positive for orthopaedic stainless steel (sample B) than for AISI 304 stainless steel (sample A), i.e., E_b is 0.32 V for sample B and 0.20 V for sample A.

Potentiodynamic curves for both stainless steels in the presence of 0.05 M citric acid and EDTA are presented in Figs. 2 and 3. The addition of complexing agents induces an increase in current density within the whole potential range and the shift of corrosion and breakdown potentials in a negative direction (Table 1). The values given represent an average value of two or three measurements. The magnitude of these changes becomes more pronounced with increasing concentration of the added agents (Table 1). The increase in current density in the lower potential range is higher for EDTA than for citric acid, whereas the current density in the passive range is similar for both complexing agents.

3.2. EIS measurements in Ringer solution

The fitting procedure was performed using equivalent circuits with simple RC elements, in series with solution resistance, R_s. The element R represents a charge transfer resistance, R_{ct}, for a kinetically-controlled electrochemical reaction at equilibrium and determines a corrosion rate. The element C represents the capacitance, C_{dl}, which exists on the interface between an electrode and its surrounding electrolyte. A simple RC element with a one time constant exhibits a characteristic semicircle in the Nyquist plot with a real part of impedance Z' on x axis, and an imaginary Z'' part on the y axis. Real components deviate from ideal behaviour in having a distribution of time constants, and impedance arcs of natural materials can deviate from a semicircular shape. The fitting procedure showed that a better agreement was obtained between experimental and theoretical data if a frequency dependent element Q (constant phase element, CPE) was introduced instead of pure capacitance. Generally, usage of a CPE is required as a result of inhomogeneities present on the microscopic level under the oxide phase and at the

Table 2 Parameter values for AISI 304 (A) and orthopaedic (B) stainless steels in Ringer solution with and without the addition of EDTA; average value of R_s were as follows: $R_s = 3.1\ \Omega\ cm^2$ for sample A and $R_s = 2.6\ \Omega\ cm^2$ for sample B in Ringer solution; $R_s = 2.6\ \Omega\ cm^2$ in 0.01 M and $R_s = 3.3\ \Omega\ cm^2$ in 0.05 M EDTA for sample A; $R_s = 2.7\ \Omega\ cm^2$ in 0.01 M and $R_s = 3.3\ \Omega\ cm^2$ in 0.05 M EDTA for sample B

	Ringer solution			Ringer solution + 0.01 M EDTA				Ringer solution + 0.05 M EDTA			
E/V	$R_{ct}/\Omega\ cm^2$	$Q \times 10^6/s^n\ \Omega^{-1}\ cm^{-2}$	*n*	$R_{ct}/\Omega\ cm^2$	$Q \times 10^6/s^n\ \Omega^{-1}\ cm^{-2}$	*n*	W/ $\Omega\ cm^2\ s^{-0.5}$	$R_{ct}/\Omega\ cm^2$	$Q \times 10^6/s^n\ \Omega^{-1}\ cm^{-2}$	*n*	W/ $\Omega\ cm^2\ s^{-0.5}$
Sample A											
−0.09	727500	40.0	0.85	600000	57.0	0.89	0.137	85997	31.0	0.96	0.123
0.22	6400	4.1	0.82	2750	1.0	1.00	—	1130	0.8	0.92	—
Sample B											
−0.09	980000	80.0	0.85	900000	20.1	0.86	—	289400	2.0	0.81	—
0.22	11480	6.8	0.85	7220	2.3	0.96	—	1750	0.6	1.00	—

oxide/electrolyte interface [33–35]. The impedance of a constant phase element is defined as [33, 34]:

$$Z_{CPE} = [Q(j\omega)^n]^{-1} \quad (1)$$

where Z is the electrode impedance, the constant Q is a combination of properties related to both the surface and the electroactive species and is independent of frequency, the exponent n is related to a slope of the log Z vs. log f in Bode plot, i.e., to the phase angle θ by the relationship $n = 2\theta/\pi$, $j = (-1)^{0.5}$. ω is the angular frequency. For $n = 1$, the Q element reduces to a capacitor with capacitance C and, for $n = 0$, to a pure resistor. $n = 0.5$ yields Warburg impedance, which occurs when a charge carrier diffuses through a material. The parameter Q ($s^n\ \Omega^{-1}cm^{-2}$) can be converted into capacitance C ($s\ \Omega^{-1}cm^{-2}$) when $n < 1$, which is especially important when experimental data are used to determine quantitatively system parameters such as thickness or dielectric constant [36]. In the present work, no calculation of C was performed since the calculated values of Q were used mostly for comparison purposes between samples in various solutions.

Impedance data were recorded for both materials at two potentials of interest, at −0.09 V in the passive range and at 0.22 V in the passive–transpassive range. The results are presented in Figs. 4 and 5 as the complex plane plots of imaginary impedance Z'' vs. real impedance Z', and the calculated parameters are presented in Table 2. According to the polarization curve, at −0.09 V the surface of AISI 304 stainless steel gradually becomes passive, as demonstrated by a relatively high R_{ct} value (Fig. 4, Table 2). At the same potential the orthopaedic steel also shows a passivation semicircle with high R_{ct} value. At 0.22 V the values of R_{ct} and Q decreased compared to values obtained at −0.09 V due to a gradual passive–transpassive transition in this potential range (Fig. 5). The difference in impedance value for both samples is markedly demonstrated with orthopaedic stainless steel having higher R_{ct} values thus exhibiting a higher

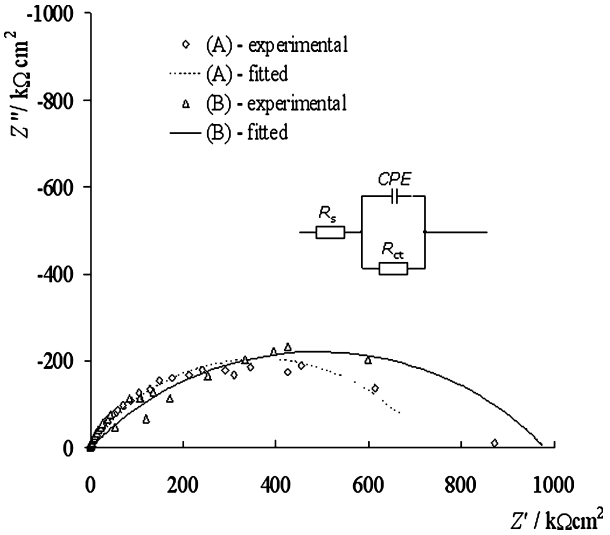

Fig. 4 Impedance spectra recorded for AISI 304 (A) and orthopaedic (B) stainless steels in Ringer physiological solution at −0.09 V vs. SCE.

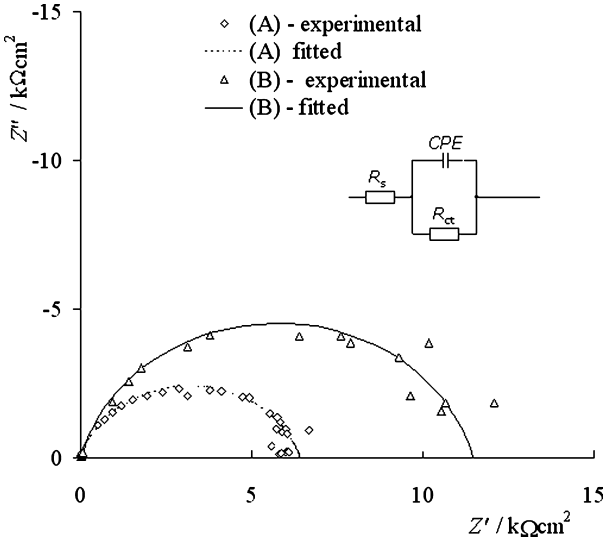

Fig. 5 Impedance spectra recorded for AISI 304 (A) and orthopaedic (B) stainless steels in Ringer physiological solution at 0.22 V vs. SCE.

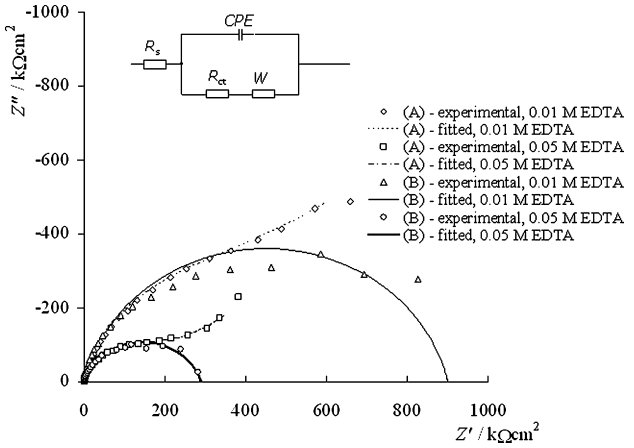

Fig. 6 Impedance spectra recorded at −0.09 V vs. SCE in the passive region for AISI 304 (A) and orthopaedic (B) stainless steels in Ringer physiological solution containing EDTA.

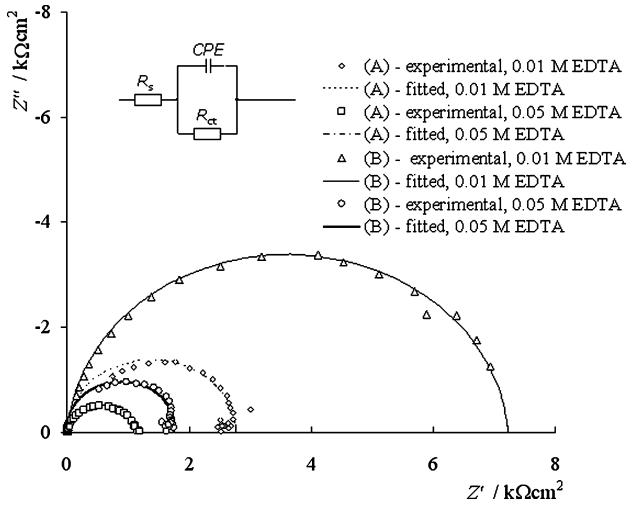

Fig. 7 Impedance spectra recorded at 0.22 V vs. SCE in the passive-transpassive region for AISI 304 (A) and orthopaedic (B) stainless steels in Ringer physiological solution containing EDTA.

corrosion resistance in physiological solution. The values of n between 0.8 and 1.0 are obtained.

Values of Q gradually decreased with increasing potential in pure Ringer solution (Table 2). In our former work [37] we suggested that the capacitance value in passive state can be a criterion for the dynamics of the chemical–adsorption processes including bond water [38]. It increases with the intensity of the dynamics. As the potential becomes more positive and reaches 0.22 V, the value of Q decreases, indicating the increase in passive layer thickness.

3.3. EIS measurements in Ringer solution containing EDTA

Impedance data recorded at −0.09 V and 0.22 V in the presence of 0.01 M and 0.05 M EDTA are presented in Figs. 6 and 7 as complex plane plots of Z'' vs. Z'. The calculated parameters are given in Table 2. The impedance plot recorded for AISI 304 stainless steel at low frequencies shows a deviation from the semicircle with involvement of diffusion process (Fig. 6). Warburg coefficients of 0.137 Ω cm^2 s$^{-0.5}$ and 0.123 Ω cm^2 s$^{-0.5}$ are determined in the presence of 0.01 M and 0.05 M EDTA, respectively, probably related to the diffusion of metal complexes to/away from the electrode surface. Compared to pure Ringer solution, the values of R_{ct} markedly decrease with increasing concentration of EDTA, thus indicating a consequent decrease in the corrosion resistance (Table 2). At the same time the value of Q decreases as well. Due to the beneficial effect of Mo, orthopaedic stainless steel shows typical semicircular impedance spectra with values of R_{ct} higher than that measured for AISI 304 stainless steel (Fig. 4, Table 2).

The addition of 0.01 M EDTA only slightly decrease the values of R_{ct}, whereas the addition of higher EDTA concentration, markedly affects the values of R_{ct} which drop more than six times compared to Ringer solution. The magnitude of R_{ct} drop is smaller for orthopaedic stainless steel – approximately three times, which indicates that this alloy is less sensitive to the presence of additives in solution.

Impedance spectra recorded at 0.22 V in the passive – transpassive region are presented in Fig. 7. Typical semicircular shapes are obtained, with values of resistance decreasing significantly compared to those in the passive region (Table 2). For both stainless steels the magnitude of R_{ct} drop amounts to two times and up to seven times for 0.01 M and 0.05 M EDTA, respectively.

3.4. EIS measurements in Ringer solution containing citric acid

Impedance data recorded at −0.09 V and 0.22 V in the presence of 0.01 M and 0.05 M citric acid are presented in Figs. 8 and 9 as the complex plane plots of Z'' vs. Z'. The calculated parameters are given in Table 3. At −0.09 V the resistance of AISI 304 stainless steel decrease by the addition of citric acid, i.e. from 727 kΩ cm^2 in pure Ringer solution to 670 kΩ cm^2 and 295 kΩ cm^2 in Ringer solution containing 0.01 M and 0.05 M citric acid, respectively (Table 3). Again, the value of Q decreases with increasing potential and concentration of complexing agent, indicating that this effect may be related to the presence of dissolved metal complexes in the vicinity of the electrode surface. The contribution of diffusion process is indicated at low frequencies with Warburg coefficient of 2.4 Ω cm^2 s$^{-0.5}$. Similar behaviour is observed for orthopaedic stainless steel with values decreasing from 980 kΩ cm^2 in pure Ringer solution to 950 kΩ cm^2 and 430 kΩ cm^2 in Ringer solution containing 0.01 M and 0.05 M citric acid, respectively (Table 3). Warburg coefficient of 19 Ω cm^2 s$^{-0.5}$ is obtained in the presence of 0.01 M citric acid (Fig. 8).

Table 3 Parameter values for AISI 304 (A) and orthopaedic (B) stainless steels in Ringer solution with and without the addition of citric acid; average value of R_s were as follows: $R_s = 3.1\ \Omega\ cm^2$ for sample A and $R_s = 2.6\ \Omega\ cm^2$ for sample B in Ringer solution; $R_s = 3.8\ \Omega\ cm^2$ in 0.01 M and $R_s = 2.7\ \Omega\ cm^2$ in 0.05 M citric acid for sample A; $R_s = 4.6\ \Omega\ cm^2$ in 0.01 M and $R_s = 3.5\ \Omega\ cm^2$ in 0.05 citric acid for sample B

	Ringer solution			Ringer solution + 0.01 M citric acid				Ringer solution + 0.05 M citric acid			
E/V	$R_{ct}/\Omega\ cm^2$	$Q \times 10^6/s^n\ \Omega^{-1}\ cm^{-2}$	*n*	$R_{ct}/\Omega\ cm^2$	$Q \times 10^6/s^n\ \Omega^{-1}\ cm^{-2}$	*n*	W/ $\Omega\ cm^2\ s^{-0.5}$	$R_{ct}/\Omega\ cm^2$	$Q \times 10^6/s^n\ \Omega^{-1}\ cm^{-2}$	*n*	W/ $\Omega\ cm^2\ s^{-0.5}$
Sample A											
−0.09	727500	40.0	0.85	670000	46.0	0.91	2.4	295090	7.0	0.96	—
0.22	6400	4.1	0.82	5460	0.5	0.98	—	1700	0.6	0.92	—
Sample B											
−0.09	980000	80.0	0.85	950930	30.2	0.80	19.0	430000	2.0	0.81	—
0.22	11480	6.8	0.85	9250	3.1	0.95	—	2250	0.8	1.00	—

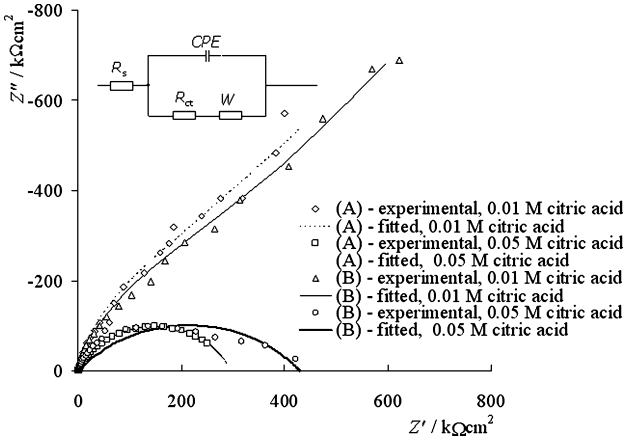

Fig. 8 Impedance spectra recorded at −0.09 V vs. SCE in the passive region for AISI 304 (A) and orthopaedic (B) stainless steels in Ringer physiological solution containing citric acid.

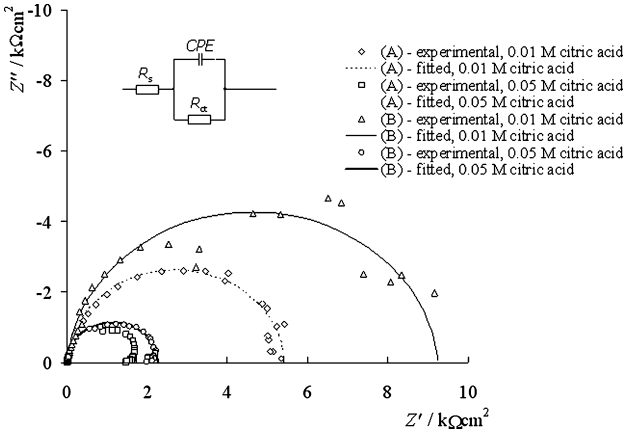

Fig. 9 Impedance spectra recorded at 0.22 V vs. SCE in the passive – transpassive region for AISI 304 (A) and orthopaedic (B) stainless steels in Ringer physiological solution containing citric acid.

At 0.22 V impedance spectra exhibit a semicircular shape with the highest value of R_{ct} found for orthopaedic stainless steel in the presence of 0.01 M citric acid, and the lowest for the AISI 304 stainless steel in 0.05 M citric acid (Fig. 9).

Again, the addition of 0.01 M citric acid only slightly affects the values of R_{ct}, whereas in the presence of 0.05 M citric acid the values of R_{ct} drop more than two times and up five times at −0.09 V and 0.22 V, respectively. Compared to EDTA, the addition of citric acid induces a smaller decrease in values of R_{ct}.

4. Discussion

The formation of passive film on iron in the rising slope of anodic peak depends strongly on the concentration of Fe^{2+} in the solution adjacent to the electrode [39]. The behaviour of stainless steel is similar, however, it has to be taken into account that the initial surface of stainless steel exposed to solution is not oxide-free but is covered by an approximately 1 nm thick layer of Cr_2O_3 spontaneously formed on its surface [2, 8]. Again, main reaction occurring at the beginning of passive region is iron oxidation. Fe(0) is oxidised to Fe_3O_4 and γ-Fe_2O_3 via Fe(II) species generated in the lower potential range [6]. At a relatively low applied potential the main species on the electrode surface are Fe_3O_4 and γ-Fe_2O_3, the fraction of the latter and other Fe(III) oxides/hydroxides, FeOOH and α-Fe_2O_3, becomes important with increasing potential. At the same time, species derived from Ni(II) and Mo(VI) build up as well [6].

Besides solid oxide film formed at the electrode surface, the formation of soluble product has to be considered in the oxidation process. Soluble Fe(II) species, or both Fe(II) and Fe(III), have been detected in alkaline solutions using rotating ring-disc electrodes [40–42]. At more negative potentials, at the initial portion of the passive region, the soluble species were identified as Fe(II), whereas in the course of further passivation and built-up of the Fe(III) oxide/hydroxide layer the soluble product changed to Fe(III) species [40, 41]. In the presence of complexing agent in the solution, complexation reactions also have to be taken into consideration. It is known from our previous experiments on individual metal

Table 4 Reactions for Fe and Ni that may be affected by the addition of complexing agents [44]

$Fe \rightarrow Fe^{2+} + 2e^-$	$E_o = 0.440 + 0.0295 \log (Fe^{2+})$	(1)
$Fe \rightarrow Fe^{3+} + 3e^-$	$E_o = 0.037 + 0.0197 \log (Fe^{3+})$	(2)
$3Fe^{2+} + 4H_2O \rightarrow Fe_3O_4 + 8H^+ + 2e^-$	$E_o = 0.980 - 0.236\ pH - 0.0886 \log (Fe^{2+})$	(3)
$2Fe^{2+} + 3H_2O \rightarrow Fe_2O_3 + 6H^+ + 2e^-$	$E_o = 0.728 - 0.1173\ pH - 0.0591 \log (Fe^{2+})$	(4)
$Ni \rightarrow Ni^{2+} + 2e^-$	$E_o = -0.250 + 0.0295 \log (Ni^{2+})$	(5)
$3Ni^{2+} + 4H_2O \rightarrow Ni_3O_4 + 8H^+ + 2e^-$	$E_o = 1.977 - 0.236\ pH - 0.0886 \log (Ni^{2+})$	(6)
$2Ni^{2+} + 3H_2O \rightarrow Ni_2O_3 + 6H^+ + 2e^-$	$E_o = 1.753 - 0.1173\ pH - 0.0591 \log (Ni^{2+})$	(7)
$Ni^{2+} + 2H_2O \rightarrow NiO_2 + 4H^+ + 2e$	$E_o = 1.593 - 0.1182\ pH - 0.0295 \log (Ni^{2+})$	(8)

components [26] that the addition of complexing agent has the highest impact on Fe and Ni, and less significant impact on Mo and Cr. This seems reasonable since although theoretically EDTA forms strong complexes with Cr^{3+} [43], this reaction is not very likely due to a high stability of Cr_2O_3. The data on stability complexes with Mo could not be found. EDTA and citrate form strong complexes with iron and nickel. The following stability constants were found for EDTA: $\log K_{st}(Fe^{2+}) = 14.3$, $\log K_{st}(Fe^{3+}) = 25.1$, $\log K_{st}(Ni^{2+}) = 18.3$, and for citrate: $\log K_{st}(Fe^{2+}) = 4.4$, $\log K_{st}(Fe^{3+}) = 11.5$ and $\log K_{st}(Ni^{2+}) = 5.3$ [43]. In the presence of these strong complexing agents the formation of metal ion complexes with chloride ions in a Ringer physiological solution becomes negligible [43]. Reactions that may be affected by the presence of complexing agents are given in Table 4 [44]. The complexation affects the equilibrium of these reactions lowering the concentration of Fe^{2+}, Fe^{3+} and Ni^{2+} in the vicinity of the electrode. Consequently, in order to preserve the equilibrium an increased dissolution of iron and nickel takes place, which is reflected in an increased current density in the potentiodynamic curves. This result was substantiated by increased concentrations of dissolved metal ions in the presence of EDTA and various proteins, as measured by differential pulse polarography (DPP) and ICP-AES [45].

EDTA induces a higher increase in current density in the lower potential range, where the formation of Fe(II) species is expected. Furthermore, it induces a higher increase in values of R_{ct}, as evident from EIS experiments. These results seem reasonable since EDTA is a stronger complexing agent for these metal ions than citric acid. Chelating of Fe^{2+} ions coming from Fe_3O_4 and γ-Fe_2O_3 barrier layer with citric acid, and especially with EDTA, prevent their oxidation, and subsequent precipitation as Fe(III) oxide. Consequently, the passive film became less protective and thinner than in the absence of complexing agent, as observed experimentally [8]. Similar results were obtained on iron metal [27] and low-carbon steel [28]. The results of impedance measurements obtained in the present work show, however, that the values of Q decrease with increasing electrode potential, although the opposite would be expected for thinning of the film in the presence of complexing compounds. We believe that this effect is more complex and may be related to the presence of a large concentration of dissolved products in the vicinity of the electrode surface, which may apparently increase the thickness of the surface layer.

The dissolution becomes more pronounced with increasing concentration of complexing agents (Table 1). For a constant potential the values of R_{ct} decrease in the following order: 0.01 M citric acid >0.01 M EDTA >0.05 M citric acid >0.05 M EDTA. Furthermore, the addition of complexing agents induces a shift in the corrosion potential (Figs. 1–3), which can be explained by the dependence of the equilibrium potential, E_o, of reactions (1–8) on the concentration of Fe^{2+}, Fe^{3+} and Ni^{2+} dissolved species (Table 4).

5. Conclusions

The electrochemical behaviour of AISI 304 and orthopaedic stainless steels differing in molybdenum content was investigated in a Ringer physiological solution with and without the addition of complexing agents. The addition of Mo has a pronounced effect on the corrosion resistance of stainless steels under physiological conditions. In polarization curves its effect was noticeable by the shift of corrosion and breakdown potentials in a more positive direction, and by the increase in R_{ct} values in EIS measurements.

The corrosion resistance of stainless steels is dependent on the type and concentration of complexing agents added to the physiological solution. In the presence of EDTA and citric acid the stability constants of the complexes between the metal and chloride ions are negligible, and thus complexes between metal ions and EDTA or citric acid prevail. Their formation causes an increased dissolution of the metal components, thereby delaying the completion of the passive film formation and, consequently, leading to decreased corrosion resistance, as evident by the values of R_{ct}. The magnitude of the R_{ct} decrease is consistent with the stability constants of related complexes, i.e., it is larger in the presence of EDTA, whose stability constants with Fe^{2+} and Ni^{2+} are significantly higher than those with citric acid. For the same complexing agent, the values of R_{ct} decrease with increasing concentration of the added agent.

Acknowledgments The authors thank Prof. Dr. Valter Doleček of the University of Maribor for valuable comments, D. Štefanec, B.Sc., for his help in the experimental work, and Prof. Dr. Miran Gaberšček of the National Institute of Chemistry for fruitful discussions. The financial support by the Slovenian Research Agency (grant No. P2–0148) is acknowledged.

References

1. E. J. SUTOW and S. R. POLLACK, In: 'Biocompatibility of Clinical Implant Materials,' vol. I, (CRC-Press, Inc., Boca Raton, Florida, 1981) p. 45.
2. N. RAMASUBRAMANIAN, N. PREOCANIN and R. D. DAVIDSON, *J. Electrochem. Soc*. **132** (1985) 793.
3. N. E. HAKIKI, M. DA CUNHA BELO, A. M. P. SIMÕES and M. G. S. FERREIRA, *J. Electrochem. Soc.* **145** (1998) 3821.
4. M. DA CUNHA BELO, N. E. HAKIKI and M. G. S. FERREIRA, *Electrochim. Acta* **44** (1999) 2473.
5. A. ROSSI and B. ELSENER, In: 'Proceedings of the 12th International Corrosion Congress', 1993, p. 2120.
6. T. PIAO and S.-M. PARK, *J. Electrochem. Soc.* **144** (1997) 3371.
7. G. LORANG, M. DA CUNHA BELO, A. M. P. SIMÕES and M. G. S. FERREIRA, *J. Electrochem. Soc.* **141** (1994) 3347.
8. I. MILOŠEV and H.-H. STREHBLOW, *J. Biomed. Mater. Res.* **52** (2000) 404.
9. R. F. A. JARGELIUS-PETTERSSON and B. G. POUND, *J. Electrochem. Soc.* **145** (1998) 1462.
10. H. OGAWA, H. OMATA, I. ITOH and H. OKADA, *Corrosion*, **34** (1978) 52.
11. J. R. GALVELE, J. B. LUMSDEN and R. W. STAEHLE, *J. Electrochem. Soc.* **125** (1978) 1204.
12. A. SCHNEIDER, D. KURON, S. HOFMANN and R. KIRCHEIM, *Corrosion Sci.* **31** (1990) 191.
13. L. WEGRELIUS and I. OLEFJORD, *Mater. Sci. Forum* **185–199** (1995) 347.
14. K. SUGIMOTO and Y. SAWADA, *Corros. Sci.* **17** (1977) 425.
15. Y. C. LU and C. R. CLAYTON, *J. Electrochem. Soc.* **133** (1986) 2465.
16. J. L. POLO, E. CANO and J. M. BASTIDAS, *J. Electroanal. Chem.* **537** (2002) 183.
17. R. BABIĆ and M. METIKOŠ–HUKOVIĆ, *J. Electroanal. Chem.* **358** (1993) 143.
18. M. A. AMEER, A. M. FEKRY and F. AL-TAIB HEAKAL, *Electrochim. Acta* **50** (2005) 43.
19. K. MEINERT and G.K. WOLF, *Surf. Coat. Technol.* **98** (1998) 1148.
20. E. LEITAO, R. A. SILVA and M. A. BARBOSA, *J. Mater. Sci.: Materials in Medicine* **8** (1997) 365.
21. C.-C. SHIH, C.-M. SHIH, Y.-Y. SU, L. H. J. SU, M.-S. CHANG and S.-J. LIN, *Corros. Sci.* **46** (2004) 427.
22. A. CIGADA, G. RONDELLI, B. VICENTINI and G. DALLASPEZIA, in Proceedings of the 12th International Corrosion Congress (1993), Houston, TX, p. 1938.
23. M. SIVAKUMAR, U. KAMCHI and S. RAJESWARI, *J. Mater. Eng. Perform.* **3** (1994) 744.
24. J. PAN, C. KARLEN and C. ULFVIN, *J. Electrochem. Soc.* **147** (2000) 1021.
25. Y. OKAZAKI, T. TATEUSHI and Y. ITO, *Mater. Trans. JIM* **38** (1997) 78.
26. I. MILOŠEV, *J. Appl. Electrochem.* **32** (2002) 311.
27. E. SIKORA and D. D. MACDONALD, *J. Electrochem. Soc.* **147** (2000) 4087.
28. S. MODIANO, C. S. FUGIVARA and A.V. BENEDETTI, *Corros. Sci.* **46** (2004) 529.
29. J. C. RUBIM, *J. Electrochem. Soc.* **140** (1993) 1601.
30. S. CATTARIN, F. FURLANETTO, M. M. MUSIANI and P. GUERRIERO, *J. Appl. Electrochem.* **24** (1994) 439.
31. Annual Book of ASTM Standards, Vol. 13.01, Medical Devices, 1988, F139–86.
32. Z. SZKLARSKA-SMIALOWSKA, In: "Pitting Corrosion of Metals" (NACE Houston, TX, 1986) p. 145.
33. B. A. BOUKAMP, In: "Equivalent Circuit Users Manual," Report CT88/265/128, University of Twente, Department of Chemical Technology, The Netherlands, 1989.
34. J. R. MACDONALD, In: "Impedance spectroscopy, emphasizing solid materials and systems" (John Wiley and Sons, New York, 1987).
35. J. S. HUEBNER and R. G. DILLENBURG, *American Mineralogist* **80** (1995) 46.
36. C. H. HSU and F. MANSFELD, *Corros. Sci.* **57** (2001) 747.
37. M. SLEMNIK, V. DOLEČEK and M. GABERŠČEK, *Acta Chim. Slov.* **49** (2002) 613.
38. G. OKAMOTO, *Corros. Sci.* **46** (1973) 471.
39. J. LIU and D. D. MACDONALD, *J. Electrochem. Soc.* **148** (2001) B425.
40. H. ZHANG and S. M. PARK, *J. Electrochem. Soc.* **141** (1994) 718.
41. S. HAUPT and H.-H. STREHBLOW, *Langmuir* **3** (1987) 873.
42. A. HUGOT LE-GOFF, J. FLIS, N. BOUCHERIT, S. JOIRET and J. WILINSKI, *J. Electrochem. Soc.* **137** (1990) 2684.
43. "Critical Stability Constants," edited by R.M. Smith, A.E. Martell (Plenum Press, New York, London, 1977) p. 163.
44. M. POURBAIX, "Atlas of Electrochemical Equilibria in Aqueous Solutions" (NACE, Cebelcor, Houston, Brussels, 1974), pp. 307, 330.
45. A. KOCIJAN, I. MILOŠEV and B. PIHLAR, *J. Mater. Sci.: Materials in Medicine* **14** (2003) 69.